

## The Effect of Particle Concentration on the Coefficient of Drag of a Spherical Particle.

D.S.Dodds<sup>1,2</sup> and J.Naser<sup>1,2</sup>

<sup>1</sup>CRC for Clean Power from Lignite  
 Mulgrave, Vic, 3170 AUSTRALIA

<sup>2</sup>School of Engineering and Science  
 Swinburne University of Technology, Vic, 3122 AUSTRALIA

### Abstract

In the simulation of dilute gas-solid flows such as those seen in many industrial applications, the Lagrangian Particle Tracking method is used to track packets of individual particles through a converged fluid field. In the tracking of these particles, the most dominant forces acting upon the particles are those of gravity and drag. In order to accurately predict particle motion, the determination of the aforementioned forces becomes of the upmost importance, and hence an improved drag force formula was developed to incorporate the effects of particle concentration. This study examines the individual effects of particles located both perpendicular and parallel to the flow direction, as well as the effect of a particle entrain within an infinite matrix of evenly distributed particles. Results show that neighbouring particles perpendicular to the flow (Model II) have an effect of increasing the drag force at close separation distances, but this becomes negligible between 5-10 particle diameters depending on particle Reynolds number ( $Re_p$ ). When entrained in an infinite line of particles co-aligned with the flow (Model I), the drag force is remarkably reduce at close separation distances and increases as the distance increases. The results of the infinite matrix of particles (Model III) show that, although not apparent in the individual model, the effect of side particles is experienced many particle diameters downstream.

### Introduction

CFD (Computational Fluid Dynamics) is utilised to model many industrial flows for a number reasons ranging from the design stage to monitoring flows where experimental measurements are unavailable. One such area is the distribution piping on a coal-fired burner as used by the coal industry in the generation of electricity. These flows consist of a carrier fluid, transporting particles from the mill to the burner outlet. Due to the low mass loadings (10%) of coal, the use Lagrangian Particle Tracking is the most appropriate, where the air flow field is solved using the full Navier-Stokes equations, and then packets of particles are individually tracked through the fluid according to Newton's 2<sup>nd</sup> law of motion. The motion of a particle is governed by the following equation:

$$m_p \frac{du_p}{dt} = \sum F \quad (1)$$

where the forces affecting the particle include the drag force and gravity force, and to a lesser extent, the added mass and Basset forces. For small particles such as those used in coal industry ( $d < 100 \mu\text{m}$ ), the drag and gravity forces become the most dominant and as such the determination of these forces is of the upmost importance in the accurate prediction of the particle phase motion.

The drag force of a spherical particle is calculated using the following theoretical formula:

$$F_D = \frac{1}{2} C_D \rho A V_{rel}^2 \quad (2)$$

where  $C_D$  is the coefficient of drag,  $A_p$  is the frontal projected area and  $V_{rel}$  is the relative velocity between the particle and the carrier fluid. The most common approach to determine the drag force on a particle is using the standard drag coefficient curve, which is based on experimental studies of a sphere in unbounded fluid flow. The most commonly accepted approximation of this curve is given by the following equation:

$$C_D = \frac{24}{Re} (1 + 0.15 Re^{0.687}) \quad Re < 1000 \quad (3)$$

As it can be seen, the above equation is solely a function of the local particle Reynolds number, and as such, discounts other effects that may affect the drag on a particle. In a situation whereby particles are relatively spread out, this assumption can be correctly employed to accurately predict particle motion, but in many industrial flows, it is impossible to assume that the distribution will be such that particles will not interact and in turn will affect each others motion. Kuan [2] found that reducing the drag coefficient to 65% of the standard  $C_D$ , predicted particle velocities better matched those of the validating experimental results of a vertical gas-particle flow. These results are based on a mass loading of 0.3, which corresponds to an average particle concentration, or particle volume fraction, of  $1.5 \times 10^{-4}$ . Although this is considered to be dilute flow, the interactions between particles cannot be ignored, which has been common practice in the past due to computer limitations and a lack of understanding of the interaction phenomenon.

A number of researchers have tried to measure the influence on the drag force of a particle in the presence of other particles [1, 3-6]. Liang [1] experimentally measured the forces in a number of particle orientations. The main findings of this research show that the drag force experienced by a particle is significantly affected by surrounding particles, more so when the particle are co-aligned. The work of Liang [1] looked at three particles co-aligned and at separation distances up to 7 particle diameters, which corresponds to a particle volume fraction of approximately  $10^{-3}$ .

It is necessary to assume that for a given particle concentration, that the particles are evenly distributed throughout the cell. Using this assumption it is possible to relate volume fraction to a uniform separation distance using the follow relation:

$$c = \frac{\pi d^3}{6L^3} \quad \text{or} \quad \frac{L}{d} = \sqrt[3]{\frac{\pi}{6c}} \quad \text{or} \quad \frac{X+d}{d} = \sqrt[3]{\frac{\pi}{6c}} \quad (4)$$

where  $c$  is the volume fraction,  $L$  is the distance between particle centres,  $X$  is the distance between particle surfaces and  $d$  is the particle diameter (See figure 1).

In order to extend this work to investigate the effects at lower concentration values,  $10^{-4}$ , which is common in many dilute phase industrial flows, a full CFD study of this work was undertaken. To gain confidence in the ability of the software to predict the trends outside of the experimental work, validation of Liang's work [1] will also be presented. The extension will include the individual effects of particle aligned both perpendicular and parallel to the flow direction, and also the final set of results will pertain to an infinite matrix of particles.

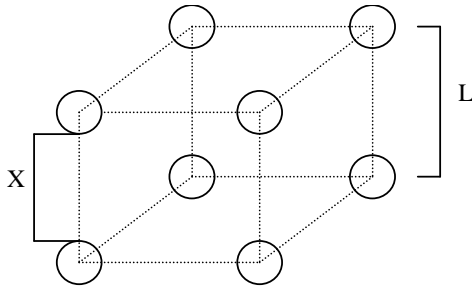


Figure 1 Particle Arrangement assuming even distribution.

### Governing Equations

As the range of Reynolds numbers of the simulated flows in this study are well within the bounds for laminar flow, the continuity and momentum equations take the forms:

$$\nabla \cdot \mathbf{U} = 0 \quad (5)$$

$$\nabla \cdot (\rho \mathbf{U} \mathbf{U}) = -\nabla p + \mu \nabla^2 \mathbf{U} \quad (6)$$

where  $\mathbf{U}$  is the velocity vector and  $p$  is the pressure. Boundary conditions will be discussed within the different models.

### Results and Discussion

#### Model Validation

In order to extend the work experimental work of Liang [1], it was necessary to simulate the published experimental results to give confidence that CFX 5.6 could accurately predict the flows and forces. The set-up consisted of three co-aligned particles of 1.58cm diameter inside a plexi-glass circular pipe of 15.24 cm diameter.

To accurately replicate the experimental conditions, a fully developed laminar pipe flow condition is used at the inlet boundary:

$$u = u_0 \left( 1 - \frac{r^2}{R^2} \right) \quad (7)$$

where  $u_0$  is the flow velocity at the centre of the pipe. No slip wall boundary conditions were applied to the particle surface and the pipe walls.

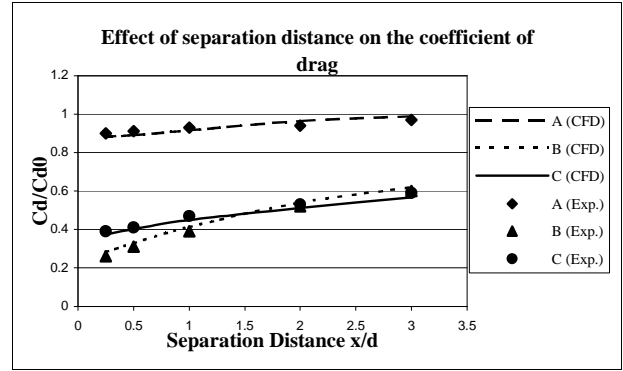


Figure 2 Validation of Liang's Experimental work at  $Re=54$

The fluid used in both the experiments and simulation was a glycerin/water solution approximately 82% glycerin with a density of  $1206 \text{ kg/m}^3$  and a viscosity of  $0.057$ . For consistency to same fluid was used for all models in this paper.

Figure 2 shows the comparison between the experimental work of Liang [1] and the CFD results where A, B and C refer to the leading, middle and trailing particles respectively. It can be seen that the present simulation quite accurately replicates the experimental results even picking up the region at a separation distance of approximately 1.5 where the middle starts to experience more drag than the trailing particle.

#### Model I.

This model contains an infinite number of particles co-aligned with the flow direction. A single particle was simulated using wall boundaries, with free slip boundary conditions, at a distance of 20 particle diameters to ensure negligible effects on the flow results. A periodic boundary condition was utilized in the stream wise direction and a body force is applied to the fluid to ensure that the momentum was conserved throughout the simulation. The fluid field was initialized with a  $u$  velocity as no inlet boundary conditions were specified. To ensure the simulation predictions were correct, this method was used to calculate the force on a isolated particle by conducting simulations with a separation distance of 60 and 80 particle diameters and compared the simulated forces with the theoretical forces using the standard approximating formula for  $C_D$ . The error difference between the CFD results and the theoretical values were within 3%, and given the fact that the formula for  $C_D$  is only an approximation it would be virtually impossible to expect any greater accuracy.

The results from this model (See Figure 3) show that at smaller separation distances, the  $C_D/C_{D0}$  ratio becomes much smaller than unity, due mainly to the fact that the fluid does not have time to return to its previously uniform state before it encounters the next particle. As the Reynolds number increases this difference becomes greater. Figure 3 shows that even up to a separation distance of 20 particle diameters, the limit of this study, that there is still a noticeable effect especially at higher Reynolds numbers.

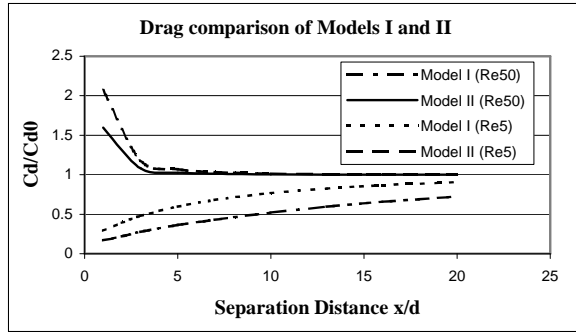


Figure 3 Comparison of Drag Coefficients for Models I and II

### Model II.

Model II consists of a single line of infinite particle along perpendicular to the flow direction. This model has been simulated using symmetry boundaries on the four walls running parallel to the flow. Although grid independency was completed for all models, Model II required a geometry independence test also. A number of different stream wise length models were tested to ensure that the drag force results were unaffected. It was found that as long as the stream wise length is at least twice as long as the separation distance, the results were unaffected. As in the stream wise direction, only a single particle was being simulated, the standard inlet and outlet boundary conditions were utilised. A uniform velocity profile was applied to the inlet boundary and a pressure boundary to the outlet. The results show that at small separation distances (See Figure 3) the drag experienced by the particle is drastically increased due to the squeezing effect of the flow as the flow area is reduced around the particle. As the coefficient of drag is highly affected by Reynolds number, it is worth noting that a lower Reynolds numbers the squeezing effect more pronounced. Depending on Re number, the effects of side neighbouring particles becomes negligible at a separation distance between 5-10 particle diameters.

### Model III.

Model III consists of a combination of Models I and II representing an infinite matrix of particles. Figure 4 shows that the effect of neighbouring particle perpendicular to flow cause a dramatic rise in the experienced drag force due to the squeezing of the flow between the particles as mentioned in Model II.

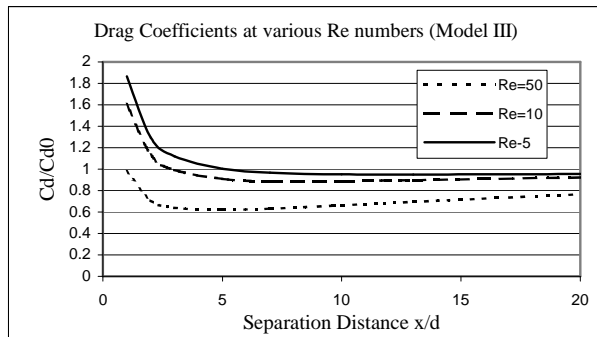


Figure 4 Drag Coefficients for Model III at Various Reynolds numbers.

Also beyond a separation distance of 5 particle diameters the  $C_D/C_{D0}$  ratio slowly approaches unity. This is due to influence of results witnessed in Model I, although it must be pointed out that the  $C_D/C_{D0}$  ratios are higher than those seen in Model I. This

difference has been highlighted in figure 5. In figure 5 the influence of Model II can be seen to be negligible but there is significance difference between Models I and III. This difference means that although not noticeable in Model II, the effects of neighbouring perpendicular particles do indeed effect the flow structure further downstream than first thought.

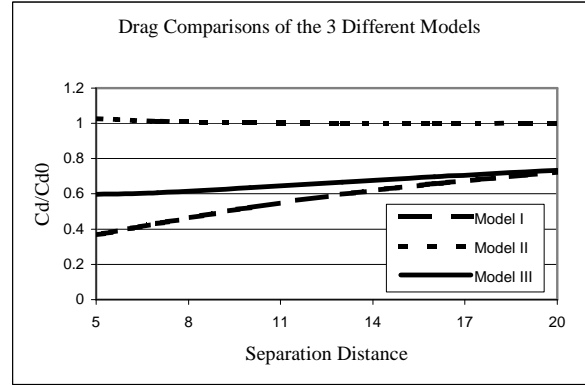


Figure 5 Comparison of the drag coefficient of the 3 models at Re=50

Figure 6 shows the normalised velocity contours of comparative simulations of Models I and III (Re = 20 and separation distance = 16d). The contours of model III carry over the squeezing effect so noticeable in the results of Model II, with the individual contours being smaller in both horizontal and vertical directions. These smaller contours mean that the average velocity in the vicinity of the particle is higher and as such we see higher drag forces experienced than those seen in Model I.

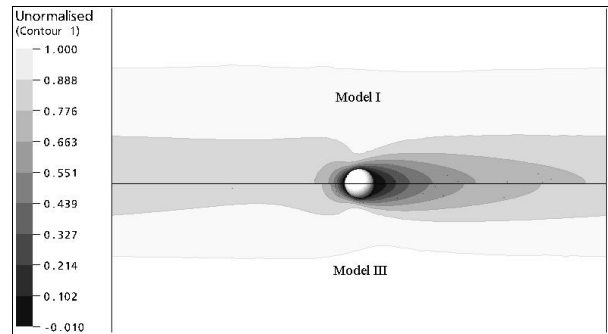


Figure 6 The Velocities at Re=20 for Models I and III

### Curve Fitting

To development of a new approximation for  $C_D$  that is a function of Reynolds number and particle volume fraction, a Least Squares Curve Fitting program was used. The generic form of the equation was chosen as:

$$C_D = \frac{24}{Re} \left( 1 + 0.15 Re^{0.687} + a \left[ \text{Log} \left( \sqrt{\frac{\pi}{6C}} \right) \right]^b + c [\text{Log}(Re)]^d \right) \quad (8)$$

where C is the particle volume fraction, Re is the local particle Reynolds number and a, b, c and d are unknown constants. Solving for these unknowns, the equation that best fits the data was found to be:

$$C_D = \frac{24}{\text{Re}} \left( 1 + 0.15 \text{Re}^{0.687} + 0.000353 \left[ \text{Log} \left( \sqrt[3]{\frac{\pi}{6C}} \right) \right]^{15.93} - 0.16 [\text{Log}(\text{Re})]^{3.62} \right) \quad (9)$$

The above is valid for re numbers ranging from 1 to 50 and particle volume fractions ranging from 0.00005 to 0.01. It is appropriate to specify these limits on the volume fraction because at higher volume fractions, the Lagrangian particle tracking is less accurate due to the lack of particle-particle interactions, which become the dominant factor in particle motion.

### Conclusion

A validating study of Liang's experimental work was conducted to test the ability of CFX 5.6 to predict flow patterns and drag forces on three co-aligned particles at several separation distances and Reynolds numbers. The study showed that the software was able to quite accurately predict the drag forces and even picked up the region highlighted in the experimental work where the middle particle began to experience more drag than the trailing particle. This validation gave confidence to extend the work to larger separation distances corresponding to lower particle volume fraction so as to develop a new coefficient of drag approximation to include the effects of volume fraction as well as Reynolds number. Three model configurations were studied to examine the individual effects of particle arrangement on the experienced drag of a particle. Model I consisted of an infinite number a co-aligned stream wise particles and results showed that a significant reduction in drag force was experienced by the particle, compared to that of an isolated particle, especially at small separation distances and higher Reynolds numbers. Model II consist of an infinite line of particles perpendicular to the flow direction. At very close separation distances, the experienced drag force increased due to increase in velocity as the flow is forced between the neighbouring particles. Beyond a separation distance of 5-7 particle diameters, the effects become negligible on the measured particle. But to the contrary when the two models were combined, forming Model III, an infinite matrix of particles, the effects of the side particles seem to have an effect on particles downstream up to 20 particles diameters

downstream. Comparing Models I and III a distinguishable difference is noticed in reduction of the drag force seen in Model I. A new approximation for the coefficient of drag for use with dilute flows has been developed according to the data of this study.

### Acknowledgements

The author gratefully acknowledges the financial and other support received for this research from the Cooperative Research Centre (CRC) for Clean Power from Lignite, which is established and supported under the Australian Government's Cooperative Research Centres program.

Also the author would to acknowledge the financial support of the Australian Postgraduate Award (APA) through Swinburne University of Technology.

### References

- [1] Liang, S.-C., Hong, T. and Fan, L.-S. Effects of Particle Arrangements on the Drag Force of a Particle in the Intermediate Flow Regime. *Int. J. Multiphase Flow*, **22**, 1996, 285-306.
- [2] Kuan, B. and Schwarz, P. Numerical prediction of particulate flows with dilute suspension in a vertical upflow circular duct: A parametric study. DMR-1930, CSIRO-Minerals, Clayton, Australia, 2002.
- [3] Lee, K. C. Aerodynamic interaction between two spheres at Reynolds numbers around  $10^4$ . *Aeronaut. Q.* **30**, 1979, 371-385.
- [4] Tsuji, Y., Morikawa, Y. & Fujiwara, Y. Pipe flow with solid particles fixed in space. *Int. J. Multiphase Flow*, **11**, 1985, 177-188.
- [5] Tsuji, Y., Morikawa, Y. & Terashima, K. Fluid-dynamic interaction between two spheres. *Int. J. Multiphase Flow*, **8**, 1982, 71-82.
- [6] Zhu, C., Liang, S.-C. & Fan, L.-S. Particle wake effects on the drag force of an interactive particle. *Int. J. Multiphase Flow*, **20**, 1994, 117-129.